Journal of Catalysis **196,** 167–173 (2000)
doi:10.1006/jcat.2000.3023, available online at http://www.idealibrary.com on IDEAL®

Infrared Study of Oxygen Adsorption and Activation on Cerium–Zirconium Mixed Oxides

C. Descorme,[1] Y. Madier, and D. Duprez

Laboratoire de Catalyse en Chimie Organique (LACCO), UMR CNRS 6503, Poitiers University, 40, Avenue du Recteur Pineau, 86022 Poitiers Cedex, France

Received May 15, 2000; revised July 27, 2000; accepted August 8, 2000

Oxygen adsorption, activation, and exchange over a wide range of $Ce_xZr_{(1-x)}O_2$ ($x = 0$, 0.15, 0.5, 0.63, and 1) mixed oxides were monitored by FT-IR spectroscopy. Oxygen adsorption at room temperature on preoxidized samples results in the formation of surface superoxides (O_2^-) that are well characterized by a sharp band at 1126 cm^{-1}. The variation along the oxide composition of the relative amount of superoxide species present at the surface, deduced from the integrated area of this ν_{O-O} vibration band, appeared to correlate with the oxygen storage capacity (OSC) of the oxide measured at 400°C. Furthermore, $^{16}O_2^-$ superoxide species adsorbed on ceria–zirconia samples were shown to be very reactive and selectively exchangeable to $^{18}O_2^-$ species via the so-called multiple exchange mechanism. The key role of superoxides as "initiators" and/or "intermediates" in the activation of oxygen prior to further diffusion on ceria-containing solids is proposed to explain the similarities observed between previous OSC measurements, $^{16}O/^{18}O$ isotopic exchange experiments, and the present FT-IR study results.

Key Words: **oxygen adsorption; oxygen activation; oxygen storage; oxygen exchange; oxygen mobility; ceria–zirconia mixed oxides; infrared; superoxides.**

1. INTRODUCTION

Ceria–zirconia mixed oxides have been intensively studied in the past few years. In 1950, Duwez and Odell established the first phase diagram of this binary system (1). Since then the structure of these mixed oxides has been widely investigated either XRD, Raman spectroscopy, and EXAFS (2–8). Until now, five different phases have been identified depending on the cerium content: one monoclinic phase, three tetragonal phases, and one cubic phase. The physicochemical properties of these solids have also been extensively studied. Along with the influence of the preparation method (9–12), the thermal stability (13–15), redox behavior (16–20), oxygen storage capacity (21–27), and oxygen mobility (28), as well as catalytic activity (29–37), were checked.

[1] To whom correspondence should be addressed. Fax: +335 49 45 34 99. E-mail: claude.descorme@campus.univ-poitiers.fr.

Despite all of those studies, only a few efforts were made to characterize the surface reactivity of these oxides. In fact, Finocchio *et al.* (38) were the only group to investigate the surface composition of mixed oxides using FT-IR with methanol as a probe molecule. CH_3OH adsorption leads to the formation of CH_3O–M^{n+} species and the frequency of the ν_{C-O} vibration band is characteristic of the M^{n+} cation. By following the thermal evolution of methoxy surface species, they evidenced the absence of surface segregation and subsequent surface enrichment in zirconium or cerium.

Looking at the surface chemistry, the aim of this preliminary study was then to identify surface oxygen species potentially involved in the oxygen storage process and to test their reactivity in the exchange pathway. Oxides under study in this paper have already been fully characterized by XRD, CO transient oxidation, and $^{18}O/^{16}O$ isotopic exchange and the results were presented in an earlier publication (28).

2. EXPERIMENTAL METHODS

2.1. OSC Measurements

OSC measurements were carried out at 400°C in a pulse chromatographic system described elsewhere (39). The sample (0.02 g) is introduced in a U-shaped fixed-bed reactor and heated to the temperature of the measurement ($10°C \cdot min^{-1}$) under flowing He ($30\ cm^3 \cdot min^{-1}$, less than 1 ppm impurities). The catalyst is then pretreated *in situ* under O_2 pulses. After 10 min of outgassing, the injection of CO pulses (loop volume $= 0.267 \pm 0.003\ cm^3$) every 2 min up to a maximum reduction of the sample (10 pulses) is followed by another 10 min of outgassing and 5 pulses of O_2. Practically, the OSC was calculated from the amount of CO_2 formed after the first CO pulse and expressed either in micromoles of CO per gram from the CO consumption or in micromoles of O per gram from the oxygen consumption.

2.2. Oxygen Isotopic Exchange

Isotopic exchange experiments were carried out in a recirculated batch reactor coupled with a quadrupole mass

0021-9517/00 $35.00

spectrometer (Balzers QMS 420). The home-made apparatus used for these studies was described in earlier publications (40–43).

On oxide-supported metals, the whole process of $^{18}O/^{16}O$ exchange occurs through a sequence of well-differentiated steps: adsorption–desorption on the metal particle, transfer from the metal to the support, and surface migration.

In the case of heteroexchange experiments, pure $^{18}O_2$ is initially introduced in the reactor and the formation of $^{18}O^{16}O$ and $^{16}O_2$ is monitored as a function of time. Strictly looking to oxygen surface migration on oxides, that is, assuming no bulk diffusion and no direct exchange, two types of heteroexchange can occur according to either Boreskov (44), Winter (45), or Novakova (46):

(i) Simple heteroexchange (type II, R^1, R'). Between one oxygen atom of a dioxygen molecule and one oxygen atom of the solid: $^{18}O_2(g) + {}^{16}O(s) \rightarrow {}^{18}O^{16}O(g) + {}^{18}O(s)$.

(ii) Multiple heteroexchange (type III, R^2, R''). Between a dioxygen molecule and two oxygen atoms of the solid: $^{18}O_2(g) + {}^{16}O^{16}O(s) \rightarrow {}^{16}O_2(g) + {}^{18}O^{18}O(s)$.

Information on the mechanism of exchange may be obtained from the relative evolution of oxygen isotopomers partial pressures at the beginning of the reaction. In fact, the formation of isotopomer 34 as a primary product indicates that exchange proceeds via a simple heteroexchange mechanism (i) while isotopomer 32 reveals a multiple exchange mechanism (ii). The type of mechanism is also expected to give some indication of the nature of mobile oxygen species.

2.3. FT-IR Spectroscopy

FT-IR spectroscopy can be used to identify surface dioxygen species formed upon oxygen adsorption and to study the reactivity of such entities during oxygen exchange reactions.

IR studies of O_2 adsorption were performed using self-supported oxide wafers (~50 mg). In order to ensure totally contaminant-free surfaces prior adsorption, the "cleaning" procedure had to be optimized in agreement with earlier studies (47). Samples were pretreated *in situ* in flowing O_2 at 400°C over 12 h in order to eliminate any remaining surface pollutants. From CO and CO_2 adsorption studies on ceria, surface contaminants were identified to be mainly carbonates (48–50). After being cleaned the IR cell is evacuated for 1 h at 400°C before adsorption studies. Spectra were collected at a resolution of 4 cm^{-1} on a Nicolet Magna 550 FT-IR spectrometer.

Two types of measurements were carried out: oxygen adsorption and surface oxygen species exchange.

Oxygen adsorption takes place at room temperature. Oxygen is introduced in the IR cell as successive doses of $^{16}O_2$, increasing the pressure from 0.5 to 20 mbar. To follow the evolution of surface oxygenated species as a function of the oxygen pressure, a spectrum is recorded at every given pressure (0.5, 1, 5, 10, and 20 mbar).

After the adsorption of oxygen ($^{16}O_2$), the exchange of the oxygenated surface species with $^{18}O_2$ may be followed by FT-IR spectroscopy to check their reactivity and get insight into the mechanism of such a process. To ensure that $^{18}O_2$ is really exchanging with surface oxygen species, and not directly adsorbing on the surface, the surface saturation in ^{16}O must be maintained before introduction of $^{18}O_2$ in the gas phase. This condition is fulfilled when the $^{16}O_2$ pressure is kept to 0.35 mbar before the introduction of $^{18}O_2$ overpressures. The exchange between $^{18}O_2$ in the gas phase and surface oxygen species is fast and increases with the $^{18}O_2$ overpressure in the IR cell. With the introduction of pure $^{18}O_2$ the total pressure is progressively increased to 0.5, 1, 5, 10, and 20 mbar. A spectrum is recorded at every given $^{18}O_2$ overpressure to follow the evolution of exchanged surface oxygen species.

All spectra presented hereafter were normalized per unit of mass. Furthermore, as the spectrum of the sample itself after pretreatment is systematically subtracted, every spectrum corresponds to the spectrum of the adsorbed phase.

3. RESULTS

3.1. Surface Oxygen Species

Surface oxygen species formed upon oxygen adsorption on $Ce_xZr_{(1-x)}O_2$ ($x = 0$, 0.15, 0.5, 0.63, and 1) at room temperature were tentatively identified by FT-IR spectroscopy.

On preoxidized mixed oxides, the formation of surface superoxide species was systematic and characterized by a very narrow band at 1126 cm^{-1}. Nevertheless, let us note that all IR spectra were acquired at room temperature. The residence time on the surface of such species at 400°C is far too short to be observed by classical FT-IR spectroscopy. Indeed, due to their very short lifetime, these species were not even detectable by EPR above 200°C.

In fact, upon O_2 adsorption on ceria, the formation of O_2^- species had already been well characterized by their O–O vibration at 1126 cm^{-1} and its overtone at 2237 cm^{-1} (51–56). Nevertheless, no such study had ever been extended to mixed oxides. Under our conditions, due to the relatively high oxygen partial pressure introduced in the cell, the influence of the oxygen partial pressure was shown to be negligible. Especially on mixed oxides, the formation of surface dioxygen species is instantaneous and complete after the introduction of the first dose of oxygen.

We observed for the first time that the population in surface superoxide species varies with the composition of the oxide. The relative amount of O_2^- species formed at the oxide surface at room temperature was quantified from the integrated area of the 1126 cm^{-1} band and normalized per unit of mass.

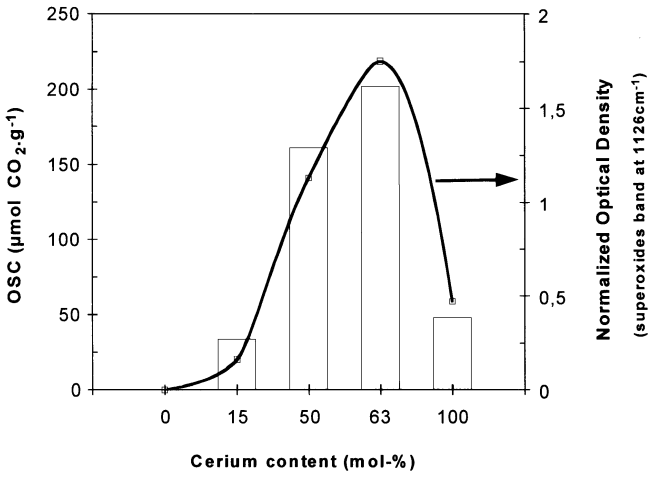

FIG. 1. Correlation between the oxygen storage capacity at 400°C and the amount of superoxides formed upon oxygen adsorption at room temperature on a series of preoxidized $Ce_xZr_{(1-x)}O_2$ mixed oxides ($x = 1$, 0.63, 0.5, 0.15, and 0).

Additionally, our previous measurements on a series of $Ce_xZr_{(1-x)}O_2$ samples had confirmed that the introduction of Zr in the ceria lattice induces an increase of the oxide OSC (28). In fact, the OSC of $Ce_{0.63}Zr_{0.37}O_2$ was measured to be 4 times larger than the OSC of ceria. An optimum was commonly observed for $Ce_xZr_{(1-x)}O_2$ oxides with x between 0.6 and 0.8 (21–28). Comparing these results, it was clear that the OSC measured at 400°C roughly varies with the population in surface dioxygen species (Fig. 1). In fact, the optimum superoxide surface coverage is observed for $Ce_{0.63}Zr_{0.37}O_2$. Therefore, it could be postulated that such O_2^- species may be involved in the oxygen transport and storage.

Furthermore, this correlation seems to indicate that the population in superoxides measured at room temperature is also representative of what is on the surface at 400°C. The only difference would be the very short lifetime of such species at 400°C.

3.2. Reactivity of Surface Oxygen Species: Correlation with Surface Mobility

It was concluded from isotopic exchange experiments that oxides may exchange their oxygen via different exchange processes (28). For example, it was shown that mixed oxides of any composition predominantly exchange their oxygen via a multiple exchange mechanism (Fig. 2B). In fact, we clearly see that, at the beginning of the exchange, the increase of mass 32 is the fastest. This observation would mean that both oxygen atoms of the dioxygen molecule are exchanged simultaneously. So, it appeared interesting to parallel the predominance of multiple exchange during isotopic exchange reactions with the presence of such binuclear oxygen species on the surface.

In this study we used FT-IR to test the reactivity of surface dioxygen species previously identified. The oxygen isotopic exchange reaction over CeO_2 and $Ce_{0.63}Zr_{0.37}O_2$ was then tentatively reproduced in the IR cell.

After the first oxygen adsorption at room temperature, two types of experiments were performed:

(i) In the first case, in order to characterize the most reactive species, surface $^{16}O_2^-$ species were directly exchanged by $^{18}O_2$ and eventually retroexchanged or back-exchanged with $^{16}O_2$. Practically, the total pressure ($^{16}O_2$) in the IR cell was reduced from 20 mbar (final adsorption pressure) to about 0.35 mbar and spectrum 1 was recorded. Overpressures of $^{18}O_2$ were then introduced in the IR cell to bring the total pressure ($^{16}O_2 + {}^{18}O_2$) to 0.5, 1, 5, 10, and 20 mbar (spectra 2 to 6).

(ii) In the second experiment, after the first set of adsorptions, the IR cell was evacuated at room temperature under high vacuum (10^{-6} mbar) for 1 h. $^{16}O_2$ was then again adsorbed ($P = 0.5$, 1, 5, 10, and 20 mbar) before exchange with $^{18}O_2$. Finally the pressure in $^{16}O_2$ was lowered to 0.35 mbar (spectrum 1) and overpressures of $^{18}O_2$ (total pressure = 0.5, 1, 5, 10, and 20 mbar) were introduced on

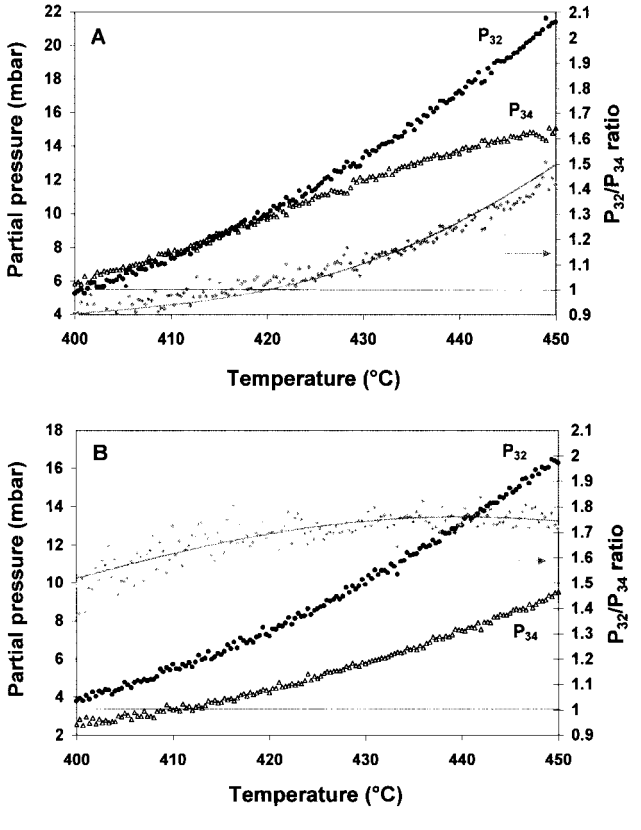

FIG. 2. Evolution of the oxygen isotopomers' partial pressures and the P_{32}/P_{34} ratio as a function of temperature in the course of a temperature-programmed $^{16}O/^{18}O$ isotopic exchange experiment (TPIE) on CeO_2 (A) and $Ce_{0.63}Zr_{0.37}O_2$ (B). Nature of the mechanism of exchange.

the sample (spectra 2 to 6). In that case only *the most stable* oxygenated species remained on the surface.

After oxygen adsorption and exchange, three different superoxide species could potentially be observed: $^{16}O_2^-$, $^{16}O^{18}O^-$, and $^{18}O_2^-$. Based on a simple theoretical calculations and earlier studies on ceria (52, 57), characteristic vibrations of $^{16}O^{18}O^-$ and $^{18}O_2^-$ are expected around 1094 cm^{-1} and 1062 cm^{-1}, respectively.

In the first set of experiments we observed that nonlabeled superoxide species ($^{16}O_2^-$) directly convert to fully labeled superoxide species $^{18}O_2^-$ (Fig. 3). In the spectrum the 1126 cm^{-1} vibration band entirely disappears in favor of a new band at 1062 cm^{-1}. Both oxide supports behave approximately in the same way with both oxygen atoms of the superoxide species being exchanged simultaneously. Nevertheless, let us recall that the amount of superoxides to be exchanged on $Ce_{0.63}Zr_{0.37}O_2$ is almost 4 times larger than that on CeO_2.

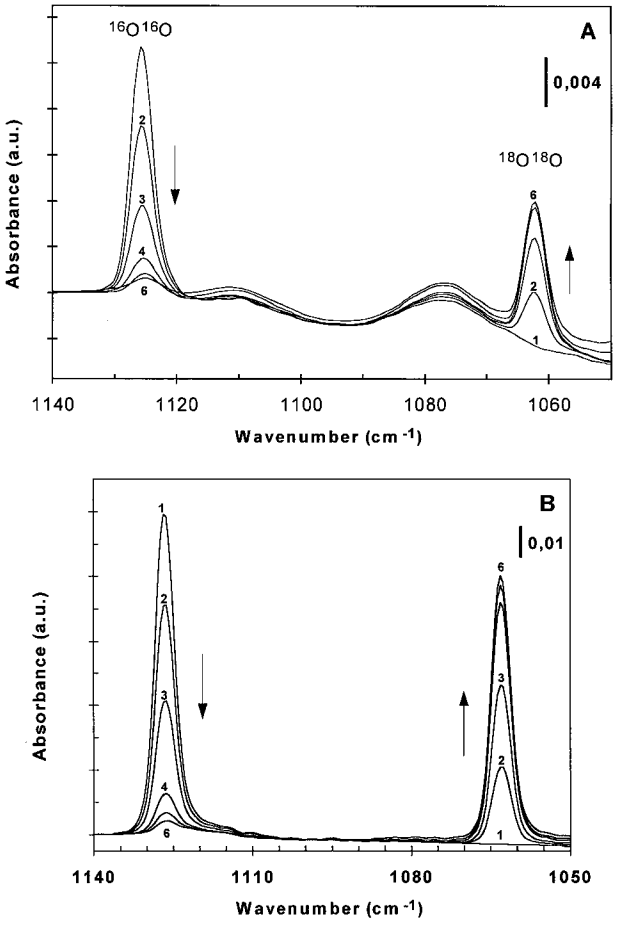

FIG. 3. IR spectral changes in the adsorbed phase on CeO_2 (A) and $Ce_{0.63}Zr_{0.37}O_2$ (B) samples upon exchange of $^{16}O_2^-$ superoxide species (spectrum 1) by gaseous $^{18}O_2$ at room temperature. Evolution as a function of $^{18}O_2$ partial pressure (spectra 2 to 6). The total pressure inside the IR cell varies from 0.5, 1, 5, 10, to 20 mbar.

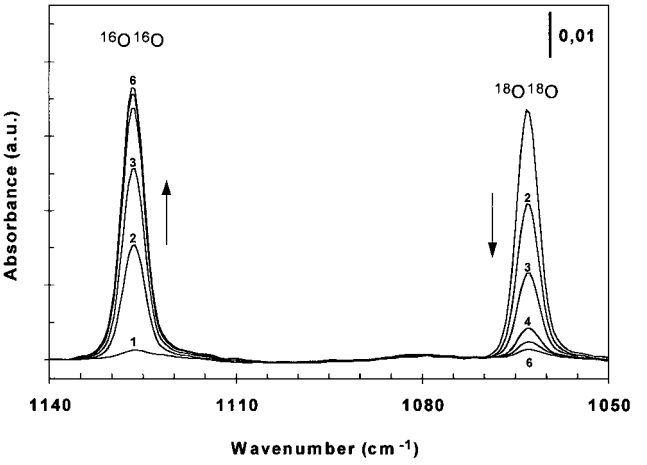

FIG. 4. IR spectral changes in the adsorbed phase on $Ce_{0.63}Zr_{0.37}O_2$ upon retroexchange of $^{18}O_2^-$ superoxide species (spectrum 1) by gaseous $^{16}O_2$ at room temperature. Evolution as a function of $^{16}O_2$ partial pressure (spectra 2 to 6). The total pressure inside the IR cell varies from 0.5, 1, 5, 10, to 20 mbar.

Furthermore, one can see on ceria that the exchange does not exclusively lead to surface $^{18}O_2^-$ species and that part of the superoxides are "lost." In fact, the subsequent formation of carbonates has been observed. The formation of such carbonate species could be the result of the interaction of carbonaceous residue from the preparation, coming back from the bulk, and oxygen or dioxygen activated species. In the case of $Ce_{0.63}Zr_{0.37}O_2$ the exchange process is more clearly reversible. In fact, even after retroexchange, almost all the 1126 cm^{-1} band intensity is recovered (Fig. 4). Almost no carbonates are formed on ceria–zirconia solids. In conclusion we could say that the most reactive surface dioxygen species exchange their oxygens via a multiple exchange mechanism.

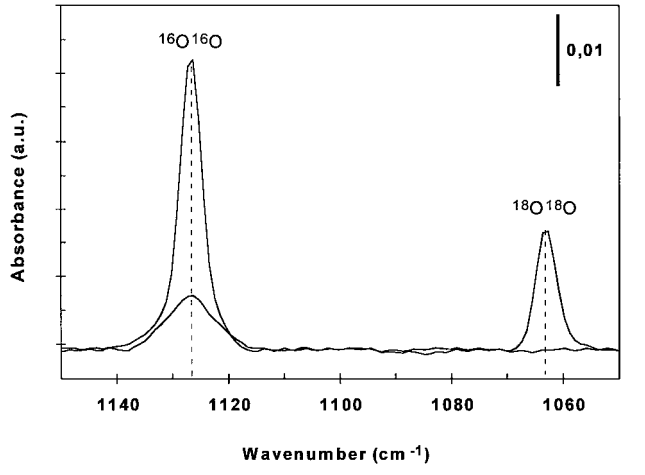

FIG. 5. IR spectral changes in the adsorbed phase on $Ce_{0.63}Zr_{0.37}O_2$ upon exchange of stable surface $^{16}O_2^-$ superoxide species (spectrum 1) by gaseous $^{18}O_2$ at room temperature (spectrum 2).

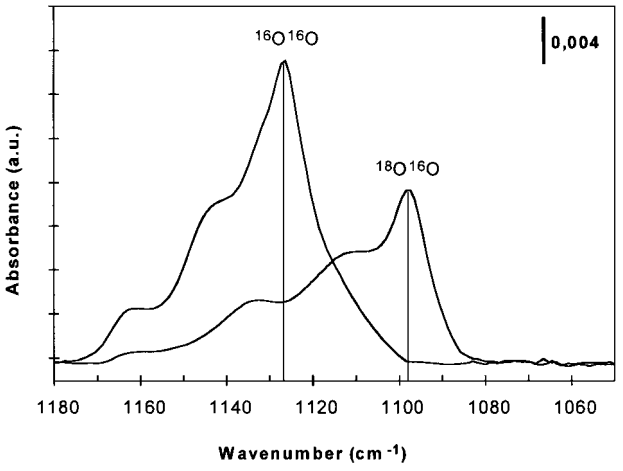

FIG. 6. IR spectral changes in the adsorbed phase on CeO_2 upon exchange of stable surface $^{16}O_2^-$ superoxide species (spectrum 1) by gaseous $^{18}O_2$ after heating at 180°C (spectrum 2).

In the course of the second type of experiment, the behavior of both samples changes drastically. On mixed oxides exchange still proceeds at room temperature via a multiple exchange mechanism. Only one new band is observed at 1062 cm^{-1} (Fig. 5). In contrast, on ceria exchange becomes more difficult and occurs only after heating of the sample to about 180°C. Furthermore, exchange takes place exclusively via a simple exchange mechanism. In fact, a new band at 1094 cm^{-1} is observed characteristic of $^{16}O^{18}O^-$ species (Fig. 6). In conclusion, even after evacuation at room temperature for 1 h, an abundant population of superoxide species exchanging oxygen via a multiple exchange mechanism still remains on the ceria–zirconia sample. In contrast, on ceria, the same "treatment" would lead to the almost complete disappearance of O_2^- species. Only a small number of "stable" superoxides, exchanging oxygen via a simple mechanism, remain on the surface. This difference between those two samples could explain their different "selectivity" in the formation of $^{18}O_2$ at the beginning of exchange during isotopic exchange experiments.

4. DISCUSSION

4.1. Oxygen Storage and Isotopic Exchange

The presence of zirconium was shown to be associated with the presence of structural defects responsible for a high oxygen mobility in these oxides and an enhanced OSC. In the cubic structure, the stress induced by the decrease of the unit cell volume, upon Ce substitution by Zr, strongly favors the formation of defects (58). In fact, Rietveld refinement of XRD spectra led to the conclusion that the number of vacancies in ceria–zirconia mixed oxides was much higher than that in pure ceria (59).

In addition, as concluded from temperature-programmed isotopic exchange experiments, the specificity of mixed oxides was shown to be the participation of bulk oxygen in the storage process (28). Calculations showed that at least one subsurface oxygen layer is involved in the storage process (22, 28).

Furthermore, it should be noticed that all of these oxides have a fluorite-type structure, which appears to be an important parameter. In the cubic phase, Zr maintains a less crowded coordination (longer metal–oxygen bonds) and as the cell parameter decreases, more and more labile oxygens are generated in the lattice (7). Indeed, Fornasiero *et al.* concluded from Raman spectroscopy studies that a tetragonalization of the cell both shortens and elongates M–O bonds and that oxygen anions move closer to octahedral sites (16). Moreover, Hagenmuller deduced from theoretical calculations that the displacement of oxygen anions toward octahedral sites would result in a more energetically favorable path for oxygen migration in the fluorite structure (60). The formation of "diffusing" channels was also proposed by Fornasiero *et al.* The channel radius was shown to have an optimum between 60 and 80 mol% in Ce (58).

4.2. Surface Oxygen Species

According to the similarities between previous isotopic exchange results and FT-IR results, it appears that binuclear oxygen species must be involved in the whole process of oxygen storage and mobility on ceria–zirconia mixed oxides. These species could be seen either as intermediates in the activation of oxygen on the oxide surface (storage) or as oxygen "carriers" throughout the oxygen surface migration process (diffusion).

To go further, the formation of surface superoxide species could potentially be explained by the interaction between molecular oxygen and a reduced cerium center (Ce^{3+}). This type of interaction would result in the reoxidation of cerium to Ce^{4+} and the subsequent formation of O_2^- species. In a more simplistic approach, this interaction could be presented as the transfer of one electron from the sample to the oxygen molecule:

$$Ce^{3+} \cdots \square + O_2 \rightarrow Ce^{4+} \cdots O_2^-.$$

In fact, notably in the case of cerium–zirconium mixed oxides, reduced centers were shown to remain in the sample even after oxidation.

Similarly, the formation of peroxide species (O_2^{2-}) on prereduced solids, observed in earlier studies (52, 56, 57), could be understood as the result of the reaction of molecular oxygen with two neighboring reduced cerium centers. In that case two electrons are transferred from the solid to the oxygen molecule, which means that the sample needs to be "deeply" reduced.

Another indication of the formation of superoxide species could be the interaction of gaseous dioxygen molecules with oxygen vacancies associated with reduced cerium

centers. Such vacancies could be structural defects or the result of the removal of oxygen anions upon reduction of the sample. In that way, dioxygen would be somehow stored in the oxygen vacancy. The parallel between the amount of superoxide species formed upon oxygen adsorption on preoxidized samples and the OSC may then become clearer.

In fact, superoxides had also been presented as "virtual" intermediates in the complete reoxidation route of CeO_{2-x}, where electrons are progressively transferred from the solid to the dioxygen molecule (56, 61):

$$O_{2gas} \rightarrow O_{2ads} \rightarrow O^-_{2ads}(\text{superoxide}) \rightarrow O^{2-}_{2ads}(\text{peroxide}) \rightarrow 2O^-_{ads} \rightarrow 2O^{2-}_{lattice}.$$

Moreover, we showed in this study that Ce/Zr oxides give rise to surface dioxygen species upon contact with oxygen in high concentrations compared to ceria. We also observed by FT-IR spectroscopy that superoxides on mixed oxides exclusively exchange through a multiple exchange mechanism. Previously, looking at the mechanism of exchange on mixed oxides by mass spectrometry, it appeared that oxygen isotopic exchange mainly proceeds via a multiple exchange mechanism (28). Furthermore, the predominance of the multiple exchange mechanism also seemed to result in a high activity in the oxygen exchange reaction. Considering these common features, the implication of superoxides in, at least, the oxygen activation process prior migration may then be underlined.

Furthermore, a thermodynamic description of defects in cerium–zirconium mixed oxides attempted by Janvier *et al.* (62) suggested that in the case of $Ce_xZr_{(1-x)}O_2$ mixed oxides, the oxygen sites at or near the surface can be greatly disturbed compared to the bulk without changing the periodicity of the structure, nor the electrical neutrality at the surface or in the bulk. The higher ability of Ce/Zr mixed oxides for oxygen storage could then be related at first to the higher concentration of oxygen vacancies at the surface. In fact, in such systems, the stabilization at or near the surface of nonstoichiometric defects in high concentrations could result in an enhanced ability to activate oxygen as superoxides. These species could thus be seen just as "initiators" of the whole storage process. The efficiency in the storage of oxygen would then be directly correlated with the concentration of vacancies at the gas/solid interface.

Moreover, these same authors showed that mainly the surface region contributes to the oxygen exchange between the gaseous phase and the oxide and that oxygen migration basically proceeds, after oxygen activation by the surface, by diffusion into the bulk via oxygen vacancies. It is further postulated that oxygen molecules are dissociated into oxygen ions before their migration into the bulk. Thus, the higher oxygen mobility of oxygen in ceria–zirconia oxides could be explained both by the enhanced ability of these oxides to activate oxygen and by the higher density of oxygen vacancies in such systems.

In conclusion, the specificity of these oxides would be their ability to activate oxygen as superoxides which seems to be the ideal initiation step for a further migration and storage of oxygen in such cerium-containing systems.

REFERENCES

1. Duwez, P., and Odell, F., *J. Am. Ceram. Soc.* **33**, 274 (1950).
2. Meriani, S., and Spinolo, G., *Powder Diffraction* **2**(4), (1987).
3. Colón, G., Pijolat, M., Valdivieso, F., Vidal, H., Kašpar, J., Finocchio, E., Daturi, M., Binet, C., Lavalley, J. C., Baker, R. T., and Bernal, S., *J. Chem. Soc., Faraday Trans.* **94**, 3717 (1998).
4. Enzo, S., Frattini, R., Delogu, F., Primavera, A., and Trovarelli, A., *Nanostructured Mater.* **12**, 673 (1999).
5. Yashima, M., Arashi, H., Kakihana, M., and Yoshimura, M., *J. Am. Ceram. Soc.* **77**(4), 1067 (1994).
6. Yashima, M., Ohtake, H., Kakihana, M., and Yoshimura, M., *J. Am. Ceram. Soc.* **77**(10), 2773 (1994).
7. Vlaic, G., Di Monte, R., Fornasiero, P., Fonda, E., Kašpar, J., and Graziani, M., *Stud. Surf. Sci. Catal.* **116**, 185 (1998).
8. Fornasiero, P., Fonda, E., Di Monte, R., Vlaic, G., Kašpar, J., and Graziani, M., *J. Catal.* **187**, 177 (1999).
9. Terribile, D., Trovarelli, A., Llorca, J., De Leitenburg, C., and Dolcetti, G., *Catal. Today* **43**, 79 (1998).
10. Masui, T., Ozaki, T., Machida, K.-I., and Adachi, G.-Y., *J. Alloys Compds.* **292**, L8 (1999).
11. Rossignol, S., Madier, Y., and Duprez, D., *Catal. Today* **50**, 261 (1999).
12. Rossignol, S., Gérard, F., and Duprez, D., *J. Mater. Chem.* **9**, 1615 (1999).
13. Janvier, C., Pijolat, M., Valdivieso, F., Soustelle, M., and Zing, C., *J. Eur. Ceram. Soc.* **18**, 1331 (1998).
14. Colón, G., Valdivieso, F., Pijolat, M., Baker, R. T., Calvino, J. J., and Bernal, S., *Catal. Today* **50**, 271 (1999).
15. Colón, G., Pijolat, M., Valdivieso, F., Baker, R. T., and Bernal, S., *in* "9th Cimtec-World Ceramics Congress—Ceramics: Getting into the 2000's" (B. Vincenzini, Ed.), Part D, p. 605. Techna Srl., 1999.
16. Fornasiero, P., Balducci, G., Di Monte, R., Kašpar, J., Sergo, V., Gubitosa, G., Ferrero, A., and Graziani, M., *J. Catal.* **164**, 173 (1996).
17. Daturi, M., Finocchio, E., Binet, C., Lavalley, J. C., Fally, F., and Perrichon, V., *J. Phys. Chem. B* **103**(23), 4884 (1999).
18. Baker, R. T., Bernal, S., Blanco, G., Cordón, A. M., Pintado, J. M., Rodríguez-Izquierdo, J. M., Fally, F., and Perrichon, V., *Chem. Commun.* 149 (1999).
19. Ozawa, M., and Loong, C.-K., *Catal. Today* **50**, 329 (1999).
20. Fornasiero, P., Kašpar, J., Sergo, V., and Graziani, M., *J. Catal.* **182**, 56 (1999).
21. Cuif, J. P., Blanchard, G., Touret, O., Seigneurin, A., Marczi, M., and Quéméré, E., "Society of Automotive Engineers Technical Paper Series," Paper No. 970463. Society of Automobile Engineers, Inc., Warrendale, PA, 1997.
22. Madier, Y., Ph.D. thesis, University of Poitiers, 1999.
23. Murota, T., Hasegawa, T., Aozasa, S., Matsui, H., and Motoyama, M., *J. Alloys Compds.* **193**, 298 (1993).
24. Cuif, J. P., Blanchard, G., Touret, O., Marczi, M., and Quéméré, E., "Society of Automotive Engineers Technical Paper Series," Paper No. 961906. Society of Automobile Engineers, Inc., Warrendale, PA, 1996.
25. Trovarelli, A., Zamar, F., Llorca, J., De Leitenberg, C., Dolcetti, G., and Kiss, J. T., *J. Catal.* **169**, 490 (1997).

26. Permana, H., Belton, D. N., Rahmoeller, K. M., Schmieg, S. J., Hori, C. E., Brenner, A., and Ng, K. Y. S., "Society of Automotive Engineers Technical Paper Series," Paper No. 970462. Society of Automobile Engineers, Inc., Warrendale, PA, 1997.
27. Finocchio, E., Daturi, M., Binet, C., Lavalley, J. C., Fally, F., Perrichon, V., Vidal, H., Kašpar, J., Graziani, M., and Blanchard, G., "Science and Technology in Catalysis," p. 257. Kodansha Ltd., 1998.
28. Madier, Y., Descorme, C., Le Govic, A. M., and Duprez, D., *J. Phys. Chem. B* **103**, 10999 (1999).
29. Di Monte, R., Fornasiero, P., Kašpar, J., Rumori, P., Gubitosa, G., and Graziani, M., *Appl. Catal. B: Environ.* **24**, 157 (2000).
30. Di Monte, R., Fornasiero, P., Kašpar, J., Ferrero, A., Gubitosa, G., and Graziani, M., *Stud. Surf. Sci. Catal.* **116**, 559 (1998).
31. Bekyarova, E., Fornasiero, P., Kašpar, J., and Graziani, M., *Catal. Today* **45**, 179 (1998).
32. Fajardie, F., Tempère, J. F., Manoli, J. M., Touret, O., Blanchard, G., and Djéga-Mariadassou, G., *J. Catal.* **179**, 469 (1998).
33. Luo, M.-F., and Zheng, X.-M., *Appl. Catal. A: General* **189**, 15 (1999).
34. Otsuka, K., Wang, Y., and Nakamura, M., *Appl. Catal. A: General* **183**, 317 (1999).
35. Pantu, P., Kim, K., and Gavalas, G. R., *Appl. Catal. A: General* **193**, 203 (2000).
36. Zhu, T., Kundakovic, L., Dreher, A., and Flytzani-Stephanopoulos, M., *Catal. Today* **50**, 381 (1999).
37. Bazin, P., Saur, O., Lavalley, J. C., Le Govic, A. M., and Blanchard, G., *Stud. Surf. Sci. Catal.* **116**, 571 (1998).
38. Finocchio, E., Daturi, M., Binet, C., Lavalley, J. C., and Blanchard, G., *Catal. Today* **52**, 53 (1999).
39. Duprez, D., *J. Chim. Phys.* **80**, 487 (1983).
40. Abderrahim, H., Ph.D. thesis, University of Poitiers, 1986.
41. Martin, D., Ph.D. thesis, University of Poitiers, 1994.
42. Abderrahim, H., and Duprez, D., *Stud. Surf. Sci. Catal.* **30**, 359 (1987).
43. Martin, D., and Duprez, D., *J. Phys. Chem.* **100**, 9429 (1996).
44. Boreskov, G., *Adv. Catal.* **15**, 285 (1964).
45. Winter, E. R. S., *J. Chem. Soc. A* 2889 (1968).
46. Novakova, J., *Catal. Rev.* **4**, 77 (1970).
47. Daturi, M., Binet, C., Lavalley, J. C., Vidal, H., Kašpar, J., Graziani, M., and Blanchard, G., *J. Chim. Phys.* **95**, 2048 (1998).
48. Li, C., Sakata, Y., Arai, T., Domen, K., Maruya, K.-Y., and Onishi, T., *J. Chem. Soc., Faraday Trans. 1* **85**(4), 929 (1989).
49. Binet, C., Jadi, A., and Lavalley, J .C., *J. Chim. Phys.* **89**, 1779 (1992).
50. Binet, C., Bradi, A., Boutonnet-Kizling, M., and Lavalley, J. C., *J. Chem. Soc., Faraday Trans.* **90**(7), 1023 (1994).
51. Li, C., Domen, K., Maruya, K.-I., and Onishi, T., *J. Chem. Soc., Chem. Commun.* 5522 (1988).
52. Li, C., Domen, K., Maruya, K.-I., and Onishi, T., *J. Am. Chem. Soc.* **111**, 7683 (1989).
53. Bozon-Verduraz, F., and Bensalem, A., *J. Chem. Soc., Faraday Trans.* **90**, 653 (1994).
54. Soria, J., Martinez-Arias, A., and Conesa, J., *J. Chem. Soc., Faraday Trans.* **91**, 1669 (1995).
55. Soria, J., Coronado, J., and Conesa, J., *J. Chem. Soc., Faraday Trans.* **92**, 1619 (1996).
56. Binet, C., Daturi, M., and Lavalley, J. C., *Catal. Today* **50**, 207 (1999).
57. Li, C., Domen, K., Maruya, K.-I., and Onishi, T., *J. Catal.* **123**, 436 (1990).
58. Fornasiero, P., Di Monte, R., Ranga Rao, G., Kašpar, J., Meriani, S., Trovarelli, A., and Graziani, M., *J. Catal.* **151**, 168 (1995).
59. Rossignol, S., Micheaud-Especel, C., and Duprez, D., *Stud. Surf. Sci. Catal.* **130**(D), 3327 (2000).
60. Hagenmuller, P., *in* "Solid Electrolytes. General Principles, Characterization, Materials, Applications, Material Science Series" (W. Vangool, Ed.). 1978.
61. Che, M., and Tench, A. J., *Adv. Catal.* **31**, 77 (1982).
62. Janvier, C., Pijolat, M., Valdivieso, F., and Soustelle, M., *Solid States Ionics* **127**, 207 (2000).